Quantum Hall effect in twisted bilayer graphene

D.S. Lee, C. Riedl, T. Beringer, K. von Klitzing, U. Starke, and J.H. Smet

The quantum Hall effect (QHE) in monolayer graphene is distinct from that of the traditional two-dimensional systems with massive electrons as a result of the linear dispersion and chiral nature of the Fermi Dirac charge carriers. Hall conductivity (σ_{xy}) quantization is observed at filling $\nu = \pm 2, \pm 6, \pm 10, \cdots$, where $\sigma_{xy} = (e^2/h)\nu$, because all Landau levels (LLs) are fourfold degenerate due to the spin and valley degrees of freedom. Moreover, the lowest LL is pinned at zero energy and its fourfold degeneracy is shared equally among holes and electrons. Bilayer graphene with AB-stacking on the other hand exhibits different Hall conductance plateaus: $\sigma_{xy} = (e^2/h)\nu_{tot}$, $\nu_{tot} = \pm 4, \pm 8, \pm 12, \cdots$. Charge carriers are still chiral, but near zero energy no longer follow a linear dispersion. They occupy a parabolic band structure due to the electronic coupling between the two layers. Because two different orbital states have both zero energy, the zero energy mode is eightfold degenerate. All other LLs are only fourfold degenerate as in a monolayer. These drastic changes in the electronic structure and the quantum Hall effect when going from a single to a bilayer of graphene, suggest that twisted bilayers are bound to exhibit rich physics as the introduction of a twist angle between the two layers away from the commensurate Bernal stacking gradually reduces the electronic coupling between the layers. How does the transition from monolayer to Bernal bilayer behavior occur? What happens to the Landau level spectrum? Here we address the quantum Hall effect in twisted bilayer graphene [1].

While the magnetotransport in twisted bilayers has remained largely unexplored, theory has extensively addressed the changes in the electronic structure. According to theory, two Dirac cones appear near the K and K'-points in the Brioullin zone with a twist angle dependent separation. The linear dispersion is preserved near zero energy. As a result of the coupling between the states of the adjacent Dirac cones, a saddle point forms in the bandstructure, which gives rise to a van Hove singularity in the density of states with a twist angle dependent van Hove energy. Moreover, the Fermi velocity gets renormalized. Even though the dispersion is still linear as in a monolayer, the eightfold degeneracy of the zero energy Landau level mode seen in commensurate Bernal graphene is topologically protected and not lost in bilayers with rotational disorder [2].

Our studies were performed on twisted bilayer graphene obtained by transferring material from the graphitized C-face of SiC. Graphene layers on this face of SiC are stacked in a turbostratic fashion with angular distributions centered around $\pm 2.2°$ and $30 \pm 2.2°$. The graphene growth was conducted by heating a 4H-SiC chip in a furnace with rf induction up to about 1300 °C. Figure 1(a) shows an atomic force microscopy (AFM) image of the sample. An adhesive tape was used to transfer the graphene layers to a Si substrate covered with a 300 nm thick oxide layer (Fig. 1(b)). Bilayers were identified from the contrast in optical microscopy. After transfer, source and drain electrodes as well as four voltage probes in the geometry seen in Fig. 1(c) were fabricated with electron beam lithography and by evaporation of Cr/Au. The turbostratic stacking of the transferred graphene layers was confirmed in Raman spectroscopy. Previous Raman studies demonstrated that the distinguishing feature between misoriented and commensurate Bernal bilayers is that for misoriented layers the 2D peak is not composed of four components, but only a single line as for monolayer graphene. The Raman data in Fig. 1(d) are in agreement with

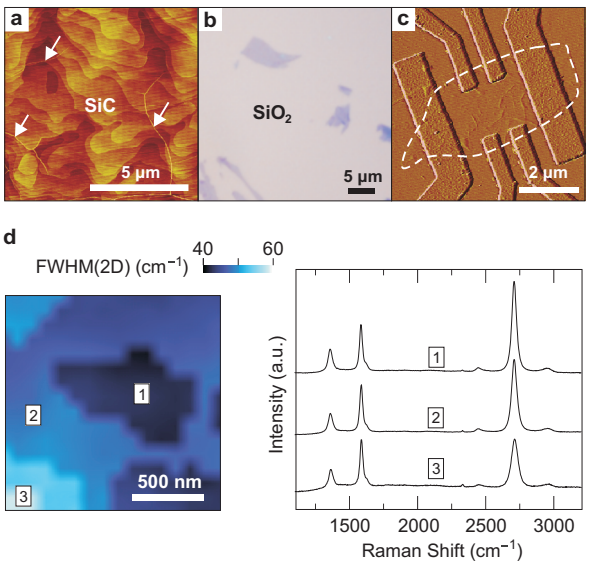

Figure 1: (a) An AFM image of multilayer epitaxial graphene grown on the C-face of SiC. (b) An optical microscope image of the graphene flakes mechanically exfoliated from SiC to SiO_2. (c) A representative AFM image of the fabricated devices. (d) Spatially resolved Raman spectra measured for the twisted bilayer flake transferred to a SiO_2 substrate. The incident light is generated by a 488 nm Ar^+ laser and the spot size is around 400 nm. The left panel shows a map of the FWHM of the 2D Raman peak. The Raman data in the right panel are the representative spectra for the different regions seen in the color rendition.

these previous observations. The 2D peak is located near 2700 cm^{-1} and fits to a single Lorentzian. We however note that the full-width-half-maximum (FWHM) of the 2D peak varies across the sample. This inhomogeneity is illustrated in the color rendition on the left. A narrowing of the 2D peak is also accompanied by a drop of the ratio of the 2D mode to G mode Raman strength (see right panel). Previous Raman studies on bilayers with rotational disorder have attributed this line width narrowing and amplitude increase to modified conditions for the double resonance process as the coupling between the graphene layers is varied and the electronic band structure changes. We conclude that the electronic coupling in our sample is position dependent.

Figure 2 shows the Hall conductivity as a function of the density induced by the back-gate voltage, $V_{\rm bg}$. The total density is calculated from $n_{\rm app} = \alpha(V_{\rm bg} - V_{\rm N})$, where $\alpha = 7.2 \times 10^{10}$ cm^{-2}V^{-1} and $V_{\rm N} = 18.5$ V is the offset voltage to reach charge neutrality. The coefficient α is known from studies on monolayers using the identical substrate. The Hall conductivity is quantized to values equal to $\sigma_{\rm xy} = i(e^2/h)$ with $i = \pm 4, \pm 8, \cdots$. This sequence is identical as for a commensurate Bernal bilayer. This can not be understood if the two layers are considered fully decoupled. If the density is assumed identical in both layers, the $8e^2/h$ plateau cannot be explained. If the densities are unequal, Hall plateaus are no longer locked to integer multiples of e^2/h.

In order to understand why the QH behavior in a twisted bilayer, despite the linear dispersion at low energy, resembles that in Bernal stacked bilayers, the LL spectrum was calculated numerically using a continuum approximation [3] and taking into account the lowest energy band of both layers. For the LL calculation we assumed the most frequently observed twist angle, $\theta = 2.2°$. Figure 2(b) displays the calculated LL spectrum. For comparison, the LL spectrum for a commensurate Bernal bilayer is also plotted in Fig. 2(c). These spectra differ substantially. The gap between the zero energy mode and the first higher or lower lying LL is much larger than the other level spacings. This is similar to the monolayer case in which the LL energy scales with $\sqrt{|n|}$ (n is the level index) due to the linear dispersion relation. At low B-fields when the LL energy is less than the van Hove energy (0.1 eV), energy levels are eightfold degenerate. In addition to the fourfold spin and valley degeneracy, there is an extra twofold degeneracy due to the split Dirac cones in twisted bilayers. This extra degeneracy is lifted at higher fields for all the LLs except for the zero mode. The eightfold degeneracy of the zero mode is topologically protected in the entire range of B [2]. Hence, for high fields the degeneracy of the LLs is the same as that for Bernal stacked bilayer: eightfold for the zero energy mode and fourfold for others. Our observation of the $\nu = 4$ and 8 QH plateau provides experimental evidence for this theoretical prediction.

Surprising are the densities at which the Hall plateaus appear. For a commensurate Bernal bilayer, the Hall transition from $4e^2/h$ to $8e^2/h$ occurs at a density near $6eB/h$. Subsequent Hall plateau transitions are equidistantly spaced with a period of $4eB/h$ because of the fourfold degeneracy of the non-zero energy LLs. In the the twisted bilayer data the transition from $4e^2/h$ to $8e^2/h$ takes place at a much larger density than $6eB/h$. Fits of the Hall conductivity at high density have been included as dashed lines in Fig. 2(a) and illustrate that these fits do not cross zero density at zero Hall conductivity. For example, at 5 T, the transition from $4e^2/h$ to $8e^2/h$ appears at $\sim 1.8 \times 10^{12}$ cm^{-2} although it is expected at $6eB/h \sim 0.7 \times 10^{12}$ cm^{-2}. In Fig. 3(a), the Hall conductivity is replotted by rescaling the $n_{\rm app}$-abscissae in units of $4eB/h$. The dashed line marks the position of the Hall transitions for a Bernal bilayer Hall plateau sequence. Clearly, the transition from $4e^2/h$ to $8e^2/h$ is "delayed". For subsequent Hall plateau transitions no additional significant shifts are observed. This behavior suggests the existence of a pool of localized states, which do not contribute to the Hall conductivity. They also do not count towards the degeneracy of the zeroth energy mode, but need to be filled in addition to all states of the zero energy mode before the next LL is broached. Apparently, the density induced by the back-gate is composed

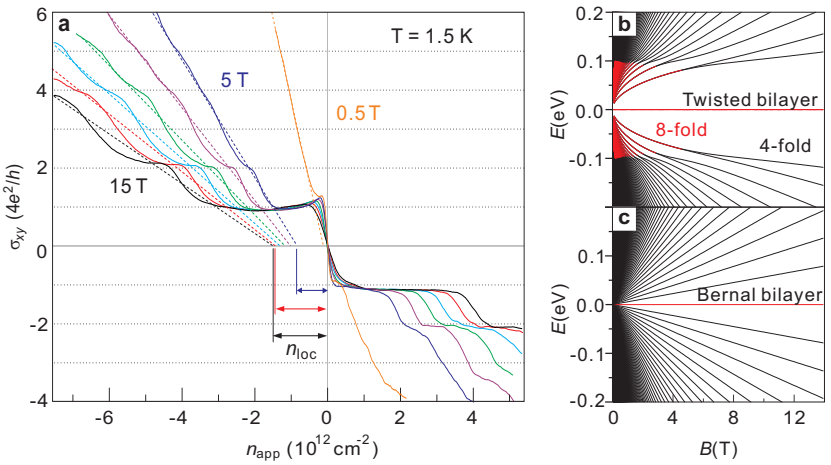

Figure 2: (a) Hall conductivity as a function of $n_{\rm app}$. (b-c) LL spectra of (b) twisted bilayer graphene and of (c) Bernal stacked bilayer graphene. The degeneracy of the energy levels is color coded: red corresponds to 8-fold degenerate and black to 4-fold degenerate.

of two contributions: $n_{\rm app} = n_{\rm tr} + n_{\rm loc}$. Here $n_{\rm tr}$ is the density that contributes to Hall transport and $n_{\rm loc}$ is the amount of localized charge that does not contribute to the Hall conductivity. When the magnetic field is altered, also $n_{\rm loc}$ changes. The localized charge $n_{\rm loc}$ has been extracted as shown in Fig. 3(a) by subtracting $6eB/h$ from the density at which the Hall conductivity changes from $4e^2/h$ to $8e^2/h$. It follows a $\sqrt{B}$ dependence (Fig. 3(b)), whereas the LL degeneracy scales linearly with B. The extracted $n_{\rm loc}$ for holes is not significantly different from that for electrons.

We attribute this unusual QH behavior to a random spatial variation of the interlayer coupling. Imagine a disordered system in which those regions where the graphene layers are weakly coupled form a continuous sea. Islands where the layers are strongly coupled are dispersed within this sea. Consider the extreme case, where the domains with strong coupling possess the LL spectrum of a commensurate Bernal bilayer, while in the weakly coupled region the spectrum resembles that of a monolayer in the sense that the LL spacing at low energies is much larger. These two spectra are plotted in Fig. 3(c). For the sake of simplicity we took the spectrum of a monolayer, although we still have some coupling. The fully decoupled scenario would be in contradiction with the observed Hall data. The more closely spaced levels in the domains with strong interlayer coupling must be filled before the second LL of the region with weak interlayer coupling gets populated. The charge carriers occupying these domains with strong interlayer coupling are localized and do not contribute to the Hall conductivity. If one assumes a parabolic band for these domains, their density can be approximated as $n_{\rm loc} = (A_{\rm coupled}/A_{\rm tot}) D_{\rm coupled} \Delta E$. Here $A_{\rm tot}$ and $A_{\rm coupled}$ are the total sample area and the area with strong interlayer coupling and $D_{\rm coupled}$ is the constant density of states at $B = 0$ in the region for strong interlayer coupling. ΔE is the energy separation between the zero energy mode and the second LL of the weakly coupled region. This energy gap scales with the $\sqrt{B}$ and hence also $n_{\rm loc}$ grows as $\sqrt{B}$. Even though this model is certainly oversimplified, it captures the dependence of $n_{\rm loc}$ on B observed in experiment (Fig. 3(c)). The question remains of whether other evidence is available for a spatially inhomogeneous coupling strength between the layers. The Raman data in Fig. 1(c) points to the existence of domains with different electronic structures. This may be a result of strain arising after growth during cool down. A non-periodic spatial variation of the electronic structure will also occur if the twist angle does not correspond to a commensurate rotation angle so that no periodic Moire pattern forms.

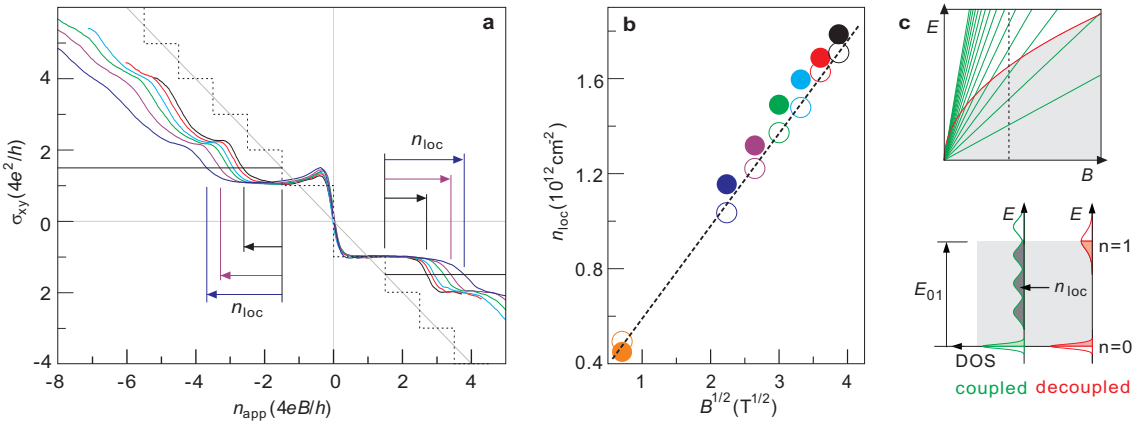

Figure 3: (a) The Hall conductivity as a function of density in units of $4eB/h$. Black dashed line: Hall conductivity for a Bernal bilayer. (b) Localized charge density $n_{\rm loc}$ for holes (open circles) and electrons (solid circles) as a function of $\sqrt{B}$. Dashed line is the linear fit of the data for holes. (c) Schematic illustration of the LLs for regions with strong and weak interlayer coupling. The energy gap between the zero mode and the next LL, E_{01} of the decoupled region is shaded in gray.

References:

[1] *Lee D.-S., T. Riedl, T. Beringer, A.H. Castro Neto, K. von Klitzing, U. Starke, J.H. Smet* Physical Review Letters **107**, 216602 (2011).

[2] *de Gail R., M.O. Goerbig, F. Guinea, G. Montambaux and A.H. Castro Neto* Physical Review B **84**, 045436 (2011).

[3] *Lopes dos Santos J.M.B., N.M.R. Peres and A.H. Castro Neto* Physical Review Letters **99**, 256802 (2007).

In collaboration with:

A.H. Castro Neto (National University of Singapore, Singapore)